Journal of Biomolecular NMR, **24:** 103–112, 2002.
KLUWER/ESCOM

NMR solution structure and dynamics of motilin in isotropic phospholipid bicellar solution

August Andersson & Lena Mäler*
Department of Biochemistry and Biophysics, Arrhenius Laboratory, Stockholm University, 10691 Stockholm, Sweden

Received 8 May 2002; Accepted 3 September 2002

Key words: ^{13}C relaxation, bicelle, dynamics, motilin, NMR, solution structure

Abstract

The structure and dynamics of the gastrointestinal peptide hormone motilin, consisting of 22 amino acid residues, have been studied in the presence of isotropic $q = 0.5$ phospholipid bicelles. The NMR solution structure of the peptide in acidic bicelle solution was determined from 203 NOE-derived distance constraints and six backbone torsion angle constraints. Dynamic properties for the $^{13}C^{\alpha}$-^{1}H vector in Leu10 were determined for motilin specifically labeled with ^{13}C at this position by analysis of multiple-field relaxation data. The structure reveals an ordered α-helical conformation between Glu9 and Lys20. The N-terminus is also well structured with a turn resembling that of a classical β-turn. The ^{13}C dynamics clearly show that motilin tumbles slowly in solution, with a correlation time characteristic of a large object. It was also found that motilin has a large degree of local flexibility as compared with what has previously been reported in SDS micelles. The results show that motilin interacts with the bicelle, displaying motional properties of a peptide bound to a membrane. In comparison, motilin in neutral bicelles seems less structured and more flexible. This study shows that the small isotropic bicelles are well suited for use as membrane-mimetic for structural as well as dynamical investigations of membrane-bound peptides by high-resolution NMR.

Introduction

Small peptides that associate with phospholipid membranes generally acquire secondary structure when bound to the membrane. However, NMR structural studies of membrane-bound peptides are difficult and usually one has to resort to the use of membrane-mimicking solvents, such as HFP or TFE, or to the use of detergent micelles to replace the role of the membrane. The use of phospholipid bicelles to mimic the membrane has recently been proposed (Sanders and Prosser, 1998; Vold et al., 1997). The bicelles used in high-resolution NMR studies are disk-shaped aggregates (Glover et al., 2001; Luchette et al., 2001) composed of long-chained phospholipids, such as dimyristoylphosphatidylcholine (DMPC), surrounded by a rim of short-chained surfactant phospholipids, such as dihexanoylphosphatidylcholine (DHPC). They form a wide range of phases as temperature, concentration and composition is varied (Gaemers and Bax, 2001; Struppe and Vold, 1998). Increasing the amount of long-chained phospholipid will result in bicelles forming a lyotropic liquid crystalline solution, widely used for determining residual dipolar couplings in weakly oriented biomolecules in such solutions (Tjandra and Bax, 1997). It has however recently been recognized that an isotropic phase exists for small [DMPC]/ [DHPC] ratios and this isotropic phase has been shown to be useful for high-resolution NMR solution studies of membrane bound peptides (Vold et al., 1997). The advantages of using the phospholipid solution instead of organics solvents or micelles are clear, as the phospholipids constitute a true membrane mimetic and do not have the same limitations that small micelles do. It has been shown that certain

*To whom correspondence should be addressed. E-mail: lena@dbb.su.se

enzymes loose their activity in micelle solution while it is retained when bound to phospholipid particles (Sanders and Landis, 1995). Structural differences for small peptides bound to micelles and phospholipid bicelles or vesicles have also been found (Chou et al., 2002; Lindberg and Gräslund, 2001; Magzoub et al., 2001). In this study we explore the use of acidic phospholipid bicelles (Struppe et al., 2000) for studying the structure and dynamics of motilin.

The linear peptide hormone motilin contains 22 amino acid residues and is present in several chordates, including *G. gallus* (chicken), *M. musculus* (mouse) and *H. sapiens* (man). It is found mainly in the gut where it stimulates the contractions of the gastrointestinal smooth muscle (Itoh, 1997). The biological effect of motilin is mediated by binding G-protein coupled motilin receptors that are associated with cell membranes. A large number of clinical and biological applications of motilin have contributed to the interest in studying the basic structure and dynamics of the peptide, in aqueous solution as well as in membrane-mimetics, to increase the knowledge about its function. The structure of motilin has been studied previously in solution containing 30% HFP (Edmondson et al., 1991; Khan et al., 1990) as well as in SDS micelle solution (Jarvet et al., 1997). The peptide studied in this report is human motilin (which has the sequence FVPIFTYGELQRMQEKERNKGQ) and it has a hydrophobic N-terminus, while the rest of the peptide is mainly hydrophilic. The peptide does not appear to have an ordered structure in aqueous solution while an α-helical structure is induced in residues 9–20 in 30% HFP and in residues 10–16 in SDS solution. In both of these structures, a wide turn is found in the N-terminal hydrophobic region.

In this study, a high-resolution solution structure based on 203 NMR-derived distance constraints has been determined in $q = 0.5$ bicelles containing a fraction of the long-chained lipids replaced by the negatively charged DMPG. In addition, the dynamic properties for the $^{13}C^{\alpha}$-^{1}H vector in Leu10 have been investigated by means of ^{13}C relaxation in both acidic as well as in neutral bicelles. The structure and dynamics are compared to previous results obtained in HFP and SDS solutions and the utility of the bicelle solution as a membrane-mimetic is discussed.

Experimental

Materials

Commercial motilin was obtained from Neosystem Labs and used as received. $^{13}C^{\alpha}$-Leu10 motilin was synthesized by the solid phase method and purified by HPLC as described previously (Allard et al., 1995). Deuterated phospholipids, dimyristoyl-*sn*-glycero-phosphatidylcholine ($^{2}H_{54}$-DMPC), dimyristoyl-*sn*-glycero-phosphatidylglycerol ($^{2}H_{54}$-DMPG) and dihexanoyl-*sn*-glycero-phosphatidylcholine ($^{2}H_{22}$-DHPC) were obtained from Avanti polar lipids. Samples containing motilin and phospholipids were produced by mixing and vortexing the peptide and long-chained phospholipid in a small amount of H_2O until a homogeneous slurry was obtained. A solution of DHPC in H_2O was added to the slurry to obtain the appropriate ratio of $q = [DMPC]/[DHPC] = 0.5$. Acidic bicelles were produced by substituting part of the DMPC by DMPG to obtain a total fraction of acidic lipids corresponding to [DMPG]/[DMPC + DMPG] = 0.3. 5% $^{2}H_2O$ was added for field/frequency lock stabilization. The total amount of lipid was around 15 w/v%, the peptide concentration was 3 mM, and the pH was adjusted to 5.5. For the sample containing the $^{13}C^{\alpha}$-Leu10 motilin, 100% $^{2}H_2O$ was used, but was otherwise treated as above.

NMR spectroscopy

All spectra were recorded using Varian Inova spectrometers, operating at 400, 600 and 800 MHz ^{1}H frequency, using a triple-resonance probe-head. All experiments were recorded at 37 °C. The temperature was calibrated using a methanol sample. Two-dimensional ^{1}H experiments were recorded at 600 MHz in pure absorption mode using the States method (States et al., 1982). The number of data points was typically 2048–4096 in the t_2 dimension and 512 in the t_1 dimension. The data processing included zerofilling to 4096 points in t_2 and 2048 in t_1 prior to Fourier transformation. In all spectra, low-power water presaturation was used to eliminate the water signal. NOESY spectra (Jeener et al., 1979) were recorded with mixing times of 100, 150 and 300 ms. TOCSY spectra (Braunschweiler and Ernst, 1983) were recorded with mixing times of 60 and 90 ms.

Inverse-detected relaxation experiments were recorded as described earlier (Allard et al., 1995; Dayie and Wagner, 1994). T_1, T_2 and steady state

NOE factors were recorded at 9.4, 14.1 and 18.8 T for the $^{13}C^{\alpha}$ of Leu10 in motilin in acidic bicelles, and at 14.1 and 18.8 T for motilin in neutral bicelles. All spectra were recorded with a minimum of 256 scans, and a minimum of ten relaxation time delays. No extra attention was given to suppression of the water signal due to the low amount of $^{1}H_2O$ in the sample. Decoupling during acquisition was performed using the GARP sequence (Shaka et al., 1985). The T_1 and T_2 data were fitted to exponentially decaying curves. The steady state NOE values were also calculated from such fits, using incremented periods of ^{1}H saturation. The errors in the measured relaxation parameters were estimated from duplicate spectra.

Structure calculation

Distance constraints were generated from quantifying NOESY cross-peaks intensities. Cross-peaks were categorized in four different bins, based on their intensities and they were given conservative upper distance limits of 3.0, 4.0, 5.0 and 6.0 Å from normalizing the intensities against known distances. The procedure was done in an iterative manner and the distance limits were adjusted in the final rounds of structure calculations. The structures were checked against the NOESY data to verify that no short distances in the structure had missing NOE connectivities in the data. However, this procedure was of limited use since many potential cross-peaks were overlapped with strong lipid signals. A total of 203 distance constraints (52 intra, 77 sequential, 63 medium and 11 long-range ($|i - j| \geqslant 5$) were obtained from the NOESY experiment ($\tau_{mix} = 100$ ms). Backbone torsion angle constraints were used for six residues in the region of the peptide identified as being helical. The basis for assigning helical torsion angle constraints was a combination of secondary chemical shift information in combination with unambiguous NOESY cross-peaks indicative of helical structure. Starting structures were generated using DIANA (Güntert et al., 1991) together with the REDAC strategy (Güntert and Wüthrich, 1991). In all, 100 starting structures were generated. These were subjected to energy minimization and restrained molecular dynamics (rMD) using the SANDER module of AMBER (Pearlmann et al., 1995). The rMD annealing cycle was 10 ps and the NMR-derived restraints were used with a force constant of 32 kcal mol^{-1} $Å^{-2}$. Out of 100 starting structures, 90 converged to produce structures with the proper stereochemistry and overall fold. A total number of 24 structures were selected to represent the solution structure and the number of structures included in the ensemble was determined using the program Findfam (Smith et al., 1996). The structures were selected based on their total and constraint energies (Mäler et al., 1999). The quality of the ensemble of final structures was checked with the program PROCHECK_NMR (Laskowski et al., 1993), to assess the stereochemistry, bond-lengths and angles, and distribution of torsion angles. Analyses of secondary structure, angles and hydrogen bonds as well as torsion and distance violations were performed with programs distributed within the GAP software package (Gippert, 1995). Root mean square deviations (rmsd) in atomic coordinates and overlays of structures were done with the program Suppose (http://www.scripps.edu/∼jsmith/suppose). Visual analyses of structures were done with Insight (MSI, version 98). The coordinates of the final structures together with the input constraints have been deposited with the Brookhaven Protein Data Bank under accession code 1LBJ and the chemical shift assignments have been deposited with the BioMagResBank under accession code 5454.

Analysis of relaxation data

The relaxation data were analyzed by modeling the spectral density function with the model-free approach (Lipari and Szabo, 1982a,b) using the Modelfree 4.01 software (Palmer et al., 1991; Mandel et al., 1995). During the fitting procedure, the scheme by Mandel et al. (1995) was used. Thus, starting from a simple model with only a global correlation time, τ_m, and an order parameter, S^2, additional parameters were added until a good fit was obtained, as defined by a statistical F-test. All parameters were fitted simultaneously, which proved important for the value of the overall correlation time. To account for effects arising from chemical exchange processes, a field-dependent exchange term, R_{ex}, was included in the expression for the R_2 relaxation rate for motilin in acidic bicelles. During the fitting of R_{ex} a two-site chemical exchange was assumed, indicating a dependence on the square of the B_0-field for fast exchange (Palmer et al., 2001). The chemical shift anisotropy was assumed to be axially symmetric, with a value of $\Delta\sigma = 25$ ppm (Cavanagh et al., 1996; Wei et al., 2001) and the ^{1}H-^{13}C inter-nuclear distance was set to 1.09 Å.

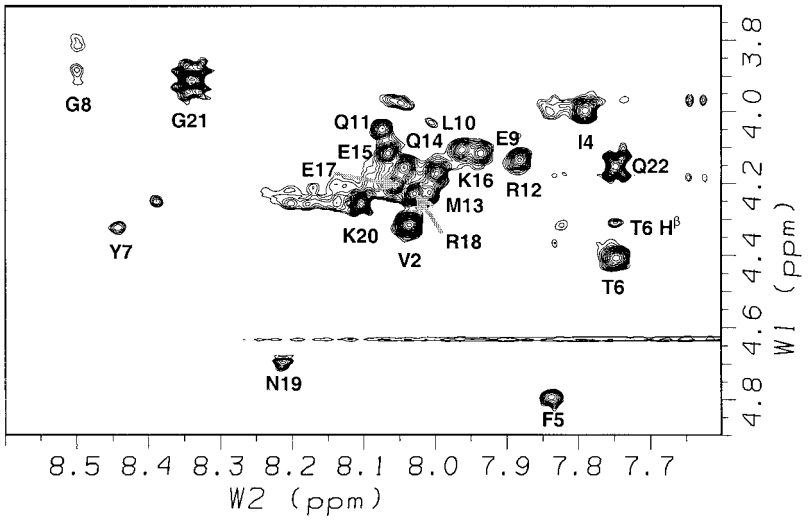

Figure 1. Part of a 600 MHz TOCSY spectrum ($\tau_{mix} = 60$ ms) for motilin in acidic phospholipid bicellar solution ($q = 0.5$, [DMPG]/[DMPC + DMPG] = 0.3) at 37 °C showing the H^N-H^α region.

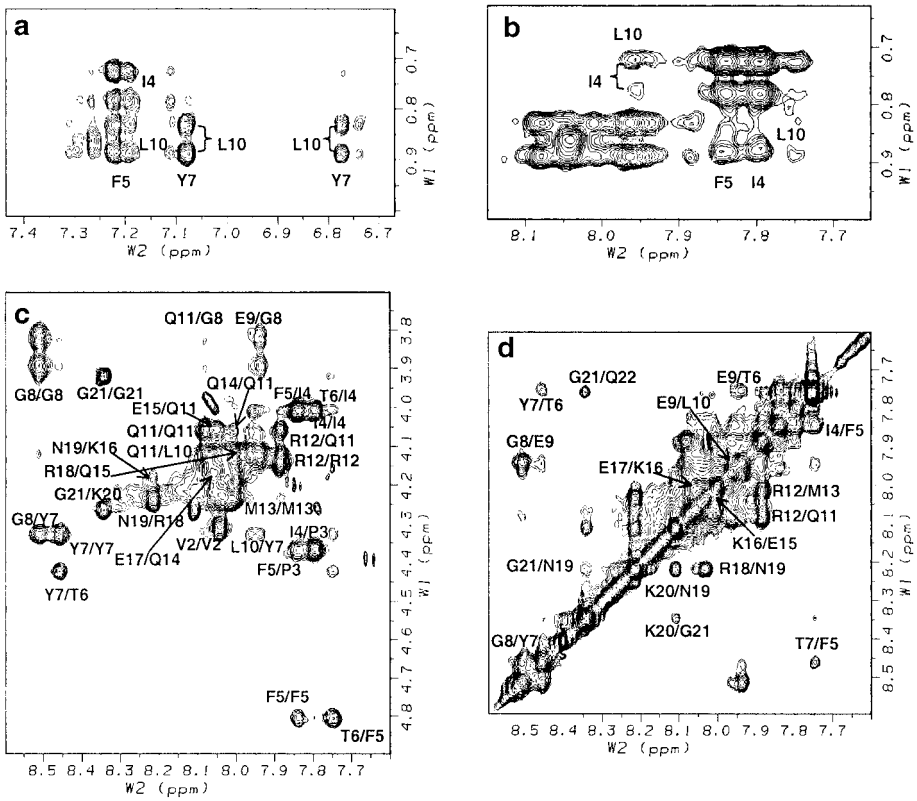

Figure 2. Details in a 600 MHz NOESY spectrum ($\tau_{mix} = 100$ ms) for motilin in acidic phospholipid bicellar solution ($q = 0.5$, [DMPG]/[DMPC + DMPG] = 0.3) at 37 °C showing (a) aromatic – methyl cross-peaks indicating unambiguous Phe5–Leu10 NOEs, (b) H^N–methyl region indicating unambiguous Ile4, Phe5–Leu10 NOEs, (c) H^N–H^α cross-peaks, (d) H^N–H^N region. Cross-peaks in (c) and (d) are indicated with their ω_2/ω_1 assignments.

Table 1. Structural statistics for motilin in bicellar solution

AMBER energies, mean and standard deviation (kcal mol^{-1})		
Constraint energy		0.54 ± 0.11
Total		-325 ± 5
Violations		
Average maximum distance violation		0.08 ± 0.01 Å
Average maximum torsion violation		$1.7 \pm 1°$
Precision, root mean square deviation (Å)		
	All heavy	Backbone
All residues	1.59	0.79
Residues 3–18	1.42	0.47
Residues in helix[a]	1.49	0.26

[a]Helix is defined between residues 9–18.

Results

Structure of motilin in bicellar solution

The structure of motilin in acidic bicellar solution was determined by the use of two-dimensional ^{1}H NMR techniques. Resonance assignments for the protons were readily obtained from analysis of TOCSY data (Figure 1) and sequential assignments were obtained from analysis of H^N-H^N and H^N-H^α connectivities in NOESY spectra (Figure 2). The chemical shifts were similar to those previously observed in SDS (Jarvet et al., 1997), with secondary chemical shifts indicative of a helical structure in the C-terminal region. Distance constraints were obtained from two-dimensional NOESY data ($\tau_{mix} = 100$ ms). Despite problems with overlap from lipid resonances, unambiguous assignments defining the α-helical region of the peptide as well as cross-peaks connecting Ile4 and Phe5 with the N-terminus of the helix (Glu9 and Leu10) could be found (Figure 2). In all, 203 NOE-derived distance constraints were used to calculate the motilin structure (Figure 3). The structure shows low molecular and constraint energies and shows good stereo-chemical properties with 84% of all residues in the most favorable regions of the Ramachandran plot, 11% in the additionally allowed regions, 4% in the generously allowed regions, and with 1% of the residues in the disallowed regions. The precision of the structure, as judged by the rmsd in atomic coordinates, is very good, with an rmsd for all backbone atoms of 0.79 Å (Table 1 and Figure 3). The structure, represented by an ensemble of 24 models is shown in Figure 4.

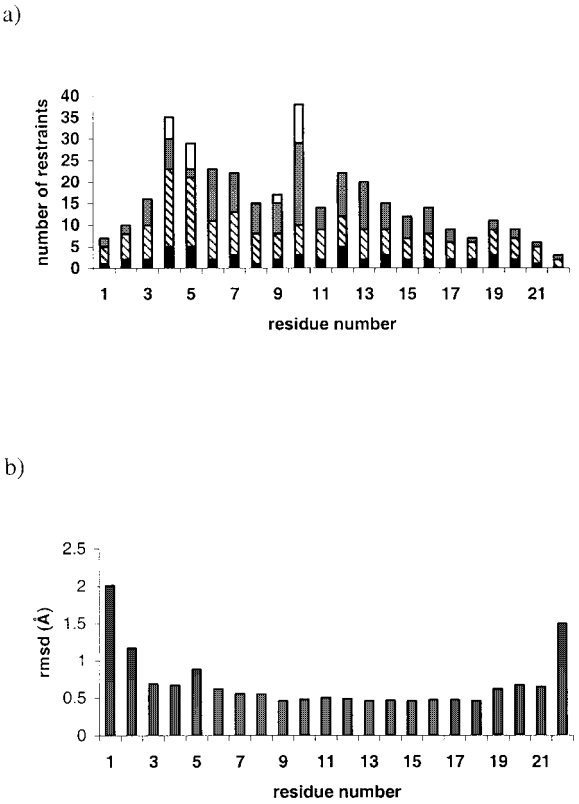

Figure 3. Plots of per residue NOE-derived distance constraints (a) and per residue rmsd in backbone atomic coordinates from the mean structure (b). The constraints are grouped into four categories: intra-residue constraints (filled), sequential constraints (hatched), medium-range constraints ($1 < |i - j| < 5$, dotted) and white long-range constraints ($|i - j| \geqslant 5$, open). All inter-residue constraints appear twice.

The secondary structure of the peptide was identified based on a combination of backbone dihedral angles and hydrogen bonding patterns. The residues at the N-terminus (Phe1 and Val2) as well as at the C-terminus (Gly21 and Gln22) are poorly defined and

Figure 4. The structure of motilin in acidic bicellar solution represented by an ensemble of 24 structures. The overlay was done by superimposing on backbone atoms in residues 3–20.

Table 2. Relaxation data for the $^{13}C^{\alpha}$-^{1}H vector of Leu10 in motilin in bicellar solution at 37 °C

B_0 (T)	R_1 (s^{-1})	R_2 (s^{-1})	NOE
Acidic bicelles			
9.39	2.84 ± 0.07	45.9 ± 1.3	1.25 ± 0.07
14.09	1.69 ± 0.03	59.1 ± 0.5	1.41 ± 0.14
18.8	1.10 ± 0.02	66.5 ± 0.8	
Neutral bicelles			
14.09	2.14 ± 0.11	20.4 ± 0.5	1.64 ± 0.19
18.8	1.61 ± 0.10	18.9 ± 1.0	

show no regular structure. An α-helical conformation was assigned to residues displaying the characteristic O_i–H^N_{i+4} hydrogen bond and with φ/ψ angles in the helical region of the Ramachandran plot. Based on these criteria, a regular α-helix could be assigned between residues Glu9 and Lys20. Four residues preceding the α-helix, Pro3–Thr6, have φ/ψ angles corresponding to a turn, resembling a β-turn of type I (Neuhaus and Williamson, 1989), where $\phi_4 = -55 \pm 19$, $\psi_4 = -58 \pm 8$, $\phi_5 = -122 \pm 6$, $\psi_5 = 30 \pm 7$. Furthermore, the expected hydrogen bond between Pro3 O and Thr6 HN is present in 19 out of 24 structures. Pro3 have φ/ψ angles corresponding to an inverse γ-turn ($\phi_3 = -79 \pm 3$, $\psi_3 = 59 \pm 12$) and a hydrogen bond between Val2 O and Ile4 HN is present in all but one structure. The structure is well defined in this region of the peptide, with an rmsd for the backbone atoms of 0.42 Å for residues Pro3–Lys20 (Table 1). In summary, motilin has a well-defined structure in the bicellar solution with the turn and helix showing low rmsds, while the termini are less well defined (Figures 3 and 4).

Dynamics in motilin

The dynamical behavior of motilin was probed by analysis of relaxation data for the Leu10 $^{13}C^{\alpha}$-^{1}H spin pair (Table 2). Relaxation data were measured at three magnetic field strengths for motilin in acidic bicelles and at two fields for motilin in neutral bicelles, and the data were analyzed with the model-free approach by Lipari and Szabo (1982a). Table 3 contains the dynamical parameters obtained from the fit for motilin in the two bicellar solutions. In both cases, it was found that a local correlation time, τ_e, was necessary for the fit. Furthermore, it was clearly observed in the

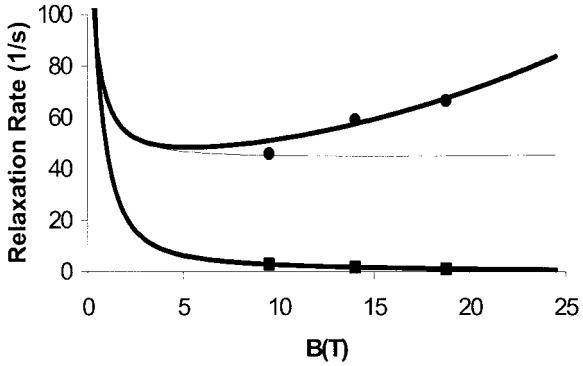

Figure 5. Relaxation data for motilin in bicellar solution. Experimentally determined R_1 values are depicted as squares, R_2 values are shown as circles. The lines are calculated relaxation rates using the model-free parameters obtained in the fit using τ_m, S^2, τ_e and R_{ex}. For the R_2 rate, the thick solid line is the calculated R_2 rate including the field dependence of R_{ex} as a function of the magnetic field strength, and the thin line is the calculated R_2 without R_{ex}.

Table 3. Model-free parameters for the $^{13}C^{\alpha}$-^{1}H vector of Leu10 in motilin at 37 °C

	τ_m (ns)	S^2	τ_e (ns)	R_{ex}
Acidic bicelles	14.2	0.69 ± 0.01	1.27 ± 0.11	5.74 ± 0.21
Neutral bicelles	7.0	0.60 ± 0.02	0.38 ± 0.07	

field-dependence of the R_2 data for motilin in acidic bicelles that a contribution from exchange influenced the measured R_2 values. Therefore an exchange term was also included in the fit, while no such term was necessary for motilin in neutral bicelles. An additional order parameter accounting for fast local motions, S^2_f, was tested (Clore et al., 1990), but was found by the use of a statistical F-test not to improve the fit. The R_1 and R_2 relaxation data together with calculated rates obtained for motilin in acidic bicelles are presented in Figure 5.

For motilin in acidic bicelles a global correlation time of $\tau_m = 14.2$ ns was obtained from the model-free analysis, which is consistent with slow overall reorientational motion, indicating that motilin is attached to a large object. The overall rotation was assumed to be isotropic during the fitting procedure, since fitting an asymmetric rotation tensor would require several investigated sites and it is unclear how to calculate such fit from the structure, since the overall rotation strongly depends on how the peptide binds the bicelle. The obtained overall reorientational correlation time should therefore be considered as an

effective correlation time, indicative of the apparent size of the peptide-bicelle complex, and of the distribution of bound and free motilin. For motilin in neutral bicelles, an effective overall correlation time of 7.0 ns was obtained, indicative of different motilin dynamics in this solvent.

During the relaxation experiments, two additional $^{13}C^{\alpha}$-^{1}H peaks appeared after a few weeks, near the motilin peak, with higher ^{1}H chemical shifts (+0.06 ppm and +0.13 ppm), and with slightly lower ^{13}C shifts (−0.52 ppm and −1.32 ppm). Both the ^{1}H and the ^{13}C chemical shifts correspond to a decrease in α-helical content. It has previously been reported that DMPG under certain conditions degrade in solution (Struppe et al., 2000) and we therefore speculate that the appearance of these motilin peaks are due to changes in bicelle composition, possibly the formation of neutral bicelles, or bicelles with a lower charge density.

Discussion

The structure of motilin has previously been determined in several solvents aimed at mimicking a membrane, such as HFP and SDS. Other structural investigations have been performed using CD and fluorescence in phospholipid vesicles (Backlund et al., 1994). One drawback of using HFP or SDS is that these solvents are known to induce α-helical conformation whereas phospholipid vesicles serve as a true membrane substitute. The phospholipid bicellar solution thus serves as a means to conduct studies of a membrane-associated peptide in a phospholipid environment by high-resolution NMR to obtain structural information on an atomic level.

In our study, the structure of motilin in acidic bicelles has been determined to ascertain the influence of the bicelles on the peptide. To further understand the influence of the solvent on the motilin structure, a comparison with the structure in SDS and in 30% HFP was made. In Figure 6, the representative structure for motilin in HFP, SDS and the family of structures in acidic bicellar solution are shown. Clearly all three structures contain α-helix conformation, although the structure in SDS seems not to contain as much α-helix as the two others do. Furthermore, the SDS structure is bent and shows poor helical properties while the present structure contains a well-defined α-helix. A similar finding has been reported, where the α-helix structure of the HIV-1 envelope peptide is curved in the presence of DHPC micelles, but is planar in the presence of bicelles (Chou et al., 2002). However, the curvature of the SDS micelle may not be enough to explain such a pronounced bend in the motilin structure. Looking at the N-terminal region, we see that a β-turn is present in all structures, although, there are differences between the structure in SDS and bicellar solution. The expected hydrogen bond is present in the motilin structure in bicelles but not in SDS, where the turn is wider than a regular β-turn of type I. The presence of the β-turn is interesting since it is the N-terminal part of the peptide that has been reported to interact with the motilin receptor (Boulanger et al., 1995). It is clear that subtle differences can be observed between the structures, and these differences may be crucial in understanding how motilin interacts with the receptor.

The dynamics data reveal important insights into the interaction between the motilin peptide and the bicelle. A global correlation time of $\tau_m = 14.2$ ns was obtained from the model-free analysis for motilin in acidic bicelles. However, it should be pointed out that if the bicelle was a rigid object with the expected size, the overall tumbling of this object would correspond to an overall correlation time on the order of 100 ns, making high-resolution NMR studies impossible (Vold et al., 1997). Therefore one might expect that the motion of lipids within the bicelle is relatively fast and unrestricted. Thus, the observed overall correlation time should be viewed as an effective correlation time for the peptide in the presence of highly mobile lipids within the bicelle. The obtained value is larger than what has been previously been reported for mastoparan interacting with neutral and acidic $q = 0.4$ bicelles (τ_m ranging from 8.0 to 10.6 ns; Whiles et al., 2001). The difference, at least in part, can be explained by differences in size and shape of the bicelles. The experimental conditions are of course not identical, but nevertheless, the global correlation time determined herein agrees well with what was found in the mastoparan study.

For motilin in neutral bicelles, a faster overall motion was observed (7.0 ns), clearly indicating that the peptide-bicelle interaction is very different in this solvent. The differences are clear already in the relaxation data, where the relaxation rates indicate different dynamics in the two solvents (Table 2). This can be explained by having more of the peptide free in solution, influencing the 'apparent' overall dynamics, or by a different interaction between motilin and the lipids, resulting in a change in bicelle composition.

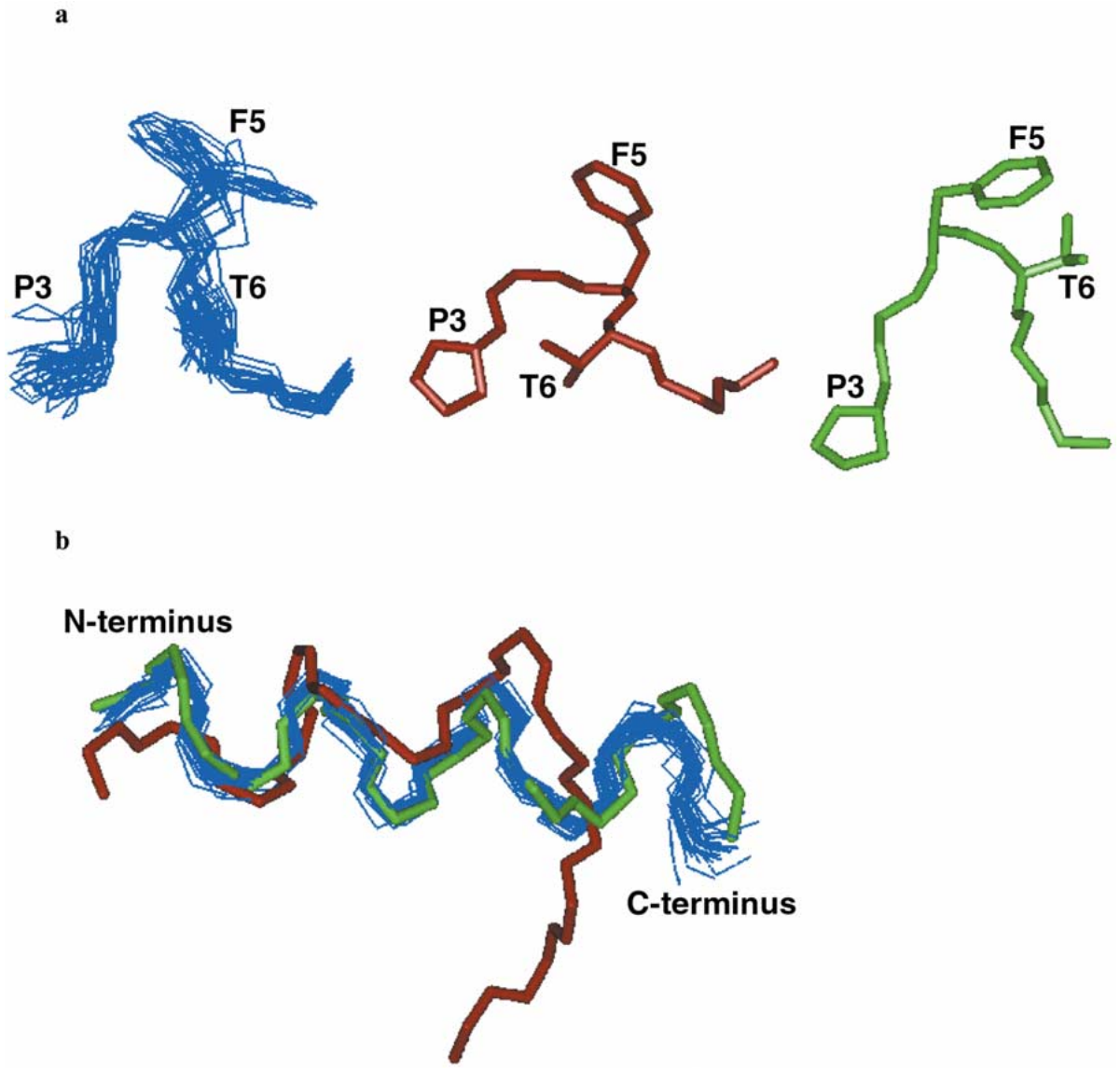

Figure 6. Structure of motilin in 30% HFP (green), SDS micelles (red) and acidic $q = 0.5$ phospholipid solution (blue). (a) Shows the N-terminal region with the β-turn and (b) shows the helix. In (a) an overlay of atomic coordinates for residues 3–8 was used and in (b) an overlay of backbone atomic coordinates for residues 8–19 was used.

Relaxation data for motilin have previously been recorded in various solvents and interpreted with the model-free approach. The dynamical parameters for motilin in ^2H_2O are $\tau_m = 1.43$ ns, $S^2 = 0.55$ and $\tau_e = 0.11$ ns corresponding to a flexible unstructured peptide (Jarvet et al., 1997). Although limited by the fact that dynamics have been obtained for one vector only, Leu10 $^{13}C^{\alpha}$-^1H, it can be noted that the local dynamics for this site become more rigid in the presence of 30% HFP ($S^2 = 0.80$, $\tau_e = 0.09$ ns) and in SDS ($S^2 = 0.92$, $\tau_e = 0.47$ ns) than in aqueous solution. The overall correlation times for the three solvents ($\tau_m = 1.43$ ns in ^2H_2O, $\tau_m = 3.06$ ns in 30% HFP and $\tau_m = 6.60$ ns in SDS) clearly reflect that the solvent induces the overall dynamical properties of motilin. In acidic bicellar solution the overall motion becomes even slower ($\tau_m = 14.2$ ns) even though the disk-shape might bias the observed τ_m. Nevertheless, the measured 'apparent' overall tumbling times for the Leu10 $^{13}C^{\alpha}$-^1H vector in different solvents are indicative of the specific peptide-solvent interactions.

Further analysis of the dynamics data reveal that motilin in acidic bicellar solution has a lower order parameter than what was found in SDS ($S^2 = 0.69$ in bicellar solution and $S^2 = 0.92$ in SDS). The order parameter is lower than what is expected for a structured protein in solution and the observed internal correlation time for motilin in acidic bicelles is somewhat long as compared to what is usually found for rigid proteins. This might be due to the fact that Leu10 is situated at the N-terminus of the helix, or that the entire helix undergoes correlated motion within the bicelle. Interestingly, this is similar to the dynamics of the amphipatic helix in the gVIIIp protein dissolved in SDS micelles (Papavoine et al., 1997). This protein folds into a conformation consisting of two α-helices, one amphipatic helix resting on the micelle surface, and a hydrophobic helix spanning the micelle. In this study, low order parameters together with nanosecond internal correlation times were found for residues in the amphipatic helix (average $S^2 = 0.51$; $\tau_e = 1.56$ ns), while high order parameters were found for residues in the hydrophobic helix. The nanosecond internal dynamics were interpreted as motion of the helix on or away from the micelle surface. When examining the distribution of hydrophobic residues in the present motilin structure it is seen that the N-terminal turn-region is mainly hydrophobic, while the α-helix is mainly hydrophilic in nature (Figure 7), suggesting that the helix mainly interacts with the surface layer of the bicelle.

It should be pointed out that it is not clear whether motilin binds to the flat membrane-like area on the bicelle or to the curved ridge. Spectra obtained for motilin in neutral bicelles show less signal dispersion indicating that the peptide is less structured in this media. Furthermore, the local dynamics for Leu10 in this solvent indicate a more flexible peptide ($S^2 = 0.60$, $\tau_e = 0.38$ ns), and, as judged by the overall dynamics in the two bicellar solvents, a different interaction between the peptide and the neutral bicelle. These findings support motilin being bound to the partially charged surface area within the acidic bicelle. It has previously been reported (Backlund et al., 1994) that motilin does not seem to obtain a helical secondary structure in vesicles composed of neutral lipids.

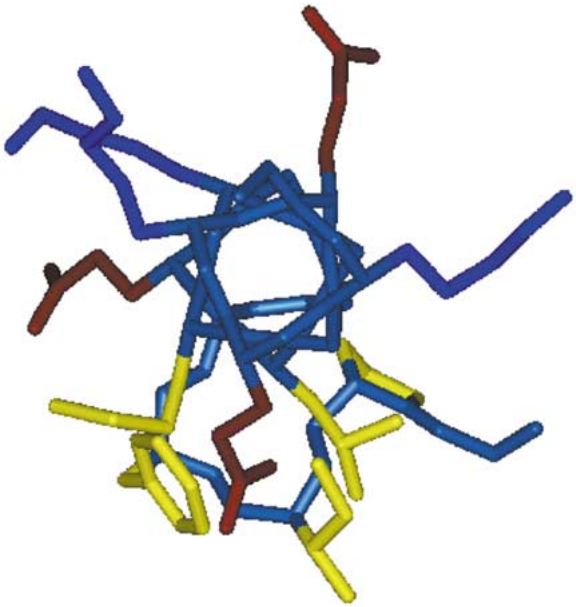

Figure 7. Distribution of charged and hydrophobic side-chains in motilin in phospholipid solution. Blue indicate basic side-chains, red acidic side-chains, and yellow hydrophobic side-chains.

Conclusions

In this study we present convincing evidence, both by structural and dynamical arguments, showing that the gastrointestinal hormone motilin binds to a negatively charged isotropic bicelle. The structure and dynamics of motilin in acidic bicelles differs from what has previously been reported for motilin in other membrane mimicking media. Residues Glu9–Lys20 adopt an ordered α-helical conformation and the N-terminus displays characteristics of two well-defined turns. Dynamics data show that motilin tumbles slowly in solution, implying that the peptide binds to the acidic bicelle and the effective overall correlation time is in agreement with what has previously been observed in bicelles. The interaction between motilin and neutral bicelles is different, and a shorter overall correlation time is observed. Since the bicelles consist of true membrane components it is therefore not far-fetched to believe that the motilin-bicelle interaction is more similar to the interaction of motilin with a real biological membrane than what is observed in the other membrane-mimicking media. Thus the results for motilin in bicelles provides new insights into the interaction between motilin and biological membranes, and also shows great potential for studying peptide-membrane interactions in general.

Acknowledgements

We thank Professor Astrid Gräslund, Drs Jüri Jarvet and Peter Damberg for valuable discussions and for supplying coordinates for the SDS and HFP motilin structures. This work was supported by the Swedish Research Council and the Carl Trygger Foundation.

References

Allard, P., Jarvet, J., Ehrenberg, A. and Gräslund, A. (1995) *J. Biomol. NMR*, **5**, 133–146.

Backlund, B.-M., Wikander, G., Peeters, T.L. and Gräslund, A. (1994) *Biochim. Biophys. Acta*, **1190**, 337–344.

Boulanger, Y., Khiat, A., Chen, Y., Gagnon, D., Poitras, P. and St-Pierre, S. (1995) *Int. J. Pept. Protein Res.*, **46**, 527–534.

Braunschweiler, L. and Ernst, R.R. (1983) *J. Magn. Reson.*, **53**, 521–528.

Cavanagh, J., Fairbrother, W.J., Palmer, A.G. and Skelton, N.J. (1996) *Protein NMR Spectroscopy*, Academic Press, San Diego.

Chou, J.J., Kaufman, J.D., Stahl, S.J., Wingfield, P.T. and Bax, A. (2002) *J. Am. Chem. Soc.*, **124**, 2450–2451.

Clore, G.M., Szabo, A., Bax, A., Kay, L.E., Driscoll, P.C. and Gronenborn, A.M. (1990) *J. Am. Chem. Soc.*, **112**, 4989–4991.

Dayie, K.T. and Wagner, G. (1994) *J. Magn. Reson. Ser.*, **A111**, 121–126.

Edmondson, S., Khan, N., Shriver, J., Zdunek, J. and Gräslund, A. (1991) *Biochemistry*, **30**, 11271–11279.

Gaemers, S. and Bax, A. (2001) *J. Am. Chem. Soc.*, **123**, 12343–12352.

Gippert, G. (1995) *New Computational Methods for 3D NMR Data Analysis and Protein Structure Determination in High-Dimensional Internal Coordinate Space*, PhD Thesis. The Scripps Institute, La Jolla.

Glover, K.J., Whiles, J.A., Wu, G., Yu, N.-J., Deems, R., Struppe, J.O., Stark, R.E., Komives, E.A. and Vold, R.R. (2001) *Biophys. J.*, **81**, 2163–2171.

Güntert, P. and Wüthrich, K. (1991) *J. Biomol. NMR*, **1**, 447–456.

Güntert, P., Braun, W. and Wüthrich, K. (1991) *J. Mol. Biol.*, **217**, 517–530.

Itoh, Z. (1997) *Peptides*, **18**, 593–608.

Jarvet, J., Zdunek, J., Damberg, P. and Gräslund, A. (1997) *Biochemistry*, **36**, 8153–8163.

Jeener, J., Meier, B.H., Bachmann, P. and Ernst, R.R. (1979) *J. Chem. Phys.*, **71**, 4546–4553.

Khan, N., Gräslund, A., Ehrenberg, A. and Shriver, J. (1990) *Biochemistry*, **29**, 5743–5751.

Laskowski, R.A., MacArthur, M.W., Moss, D.S. and Thornton, J.M. (1993) *J. Appl. Crystallogr.*, **26**, 283–291.

Lindberg, M. and Gräslund, A. (2001) *FEBS Lett.*, **497**, 39–44.

Lipari, G. and Szabo, A. (1982a) *J. Am. Chem. Soc.*, **104**, 4546–4559.

Lipari, G. and Szabo, A. (1982b) *J. Am. Chem. Soc.*, **104**, 4559–4570.

Luchette, P.A., Vetman, T.N., Prosser, R.S., Hancock, R.E.W., Nieh, M.-P., Glinka, C.J., Krueger, S. and Katsaras, J. (2001) *Biochim. Biophys. Acta*, **1513**, 83–94.

Magzoub, M., Kilk, K., Eriksson, L.E.G. and Gräslund, A. (2001) *Biochim. Biophys. Acta*, **1512**, 77–89.

Mäler, L., Potts, B.C.M. and Chazin, W.J. (1999) *J. Biomol. NMR*, **13**, 233–247.

Mandel, A.M., Akke, M. and Palmer, A.G. (1995) *J. Mol. Biol.*, **246**, 144–163.

Neuhaus, D. and Williamson, M.P. (1989) *The Nuclear Overhauser Effect in Structure and Conformational Analysis*, VCH, New York, NY.

Palmer, A.G., Kroenke, C.D. and Loria, P.J. (2001) *Meth. Enzymol.*, **339**, 204–238.

Palmer, A.G., Rance, M. and Wright, P.E. (1991) *J. Am. Chem. Soc.*, **113**, 4371–4380.

Papavoine, C.H.M., Remerowski, M.L., Horstink, L.M., Konings, R.N.H., Hilbers, C.W. and van de Ven, F.J.M. (1997) *Biochemistry*, **36**, 4015–4026.

Pearlmann, D.A., Case, D.A., Caldwell, J.W., Ross, W.S., Cheatham III, T.E., Ferguson, D.M., Seibel, G.L., Singh, U.C., Weiner, P.K. and Kollman, P.A. (1995) *AMBER 4.1*. University of California, San Fransisco, CA.

Sanders, C.R. and Landis, G.C. (1995) *Biochemistry*, **34**, 4030–4040.

Sanders, C.R. and Prosser, R.S. (1998) *Structure*, **6**, 1227–1234.

Shaka, A.J., Barker, P.B. and Freeman, R. (1985) *J. Magn. Reson.*, **64**, 547–552.

Smith, J.A., Gomez-Paloma, L., Case, D.A. and Chazin, W.J. (1996) *Magn. Reson. Chem.*, **34**, 147–155.

States, D.J., Haberkorn, R.A. and Ruben, D.J. (1982) *J. Magn. Reson.*, **48**, 286–292.

Struppe, J. and Vold, R.R. (1998) *J. Magn. Reson.*, **135**, 541–546.

Struppe, J., Whiles, J.A. and Vold, R.R. (2000) *Biophys. J.*, **78**, 281–289.

Tjandra, N. and Bax, A. (1997) *Science*, **278**, 1111–1114.

Vold, R.R., Prosser, R.S. and Deese, A.J. (1997) *J. Biomol. NMR*, **9**, 329–335.

Wei, Y., Lee, D.-K. and Ramamoorthy, A. (2001) *J. Am. Chem. Soc.*, **123**, 6118–6126.

Whiles, J.A., Brasseur, R., Glover, K.J., Melacini, G., Komives, E.A. and Vold, R.R. (2001) *Biophys. J.*, **80**, 280–293.